

Characterizing The Spatial Structure of Defensive Skill in Professional Basketball

Alexander Franks*, Andrew Miller, Luke Bornn, and Kirk Goldsberry

Alexander Franks & Luke Bornn
 1 Oxford Street, Cambridge, MA 02138
 e-mail: afranks@fas.harvard.edu

bornn@stat.harvard.edu

Andrew Miller
 33 Oxford Street, Cambridge, MA 02138
 e-mail: acm@seas.harvard.edu

Kirk Goldsberry
 1737 Cambridge Street, Cambridge, MA 02138
 e-mail: kgoldsberry@fas.harvard.edu

Abstract: Although basketball is a dualistic sport, with all players competing on both offense and defense, almost all of the sport's conventional metrics are designed to summarize offensive play. As a result, player valuations are largely based on offensive performances and to a much lesser degree on defensive ones. Steals, blocks, and defensive rebounds provide only a limited summary of defensive effectiveness, yet they persist because they summarize salient events that are easy to observe. Due to the inefficacy of traditional defensive statistics, the state of the art in defensive analytics remains qualitative, based on expert intuition and analysis that can be prone to human biases and imprecision.

Fortunately, emerging optical player tracking systems have the potential to enable a richer quantitative characterization of basketball performance, particularly defensive performance. Unfortunately, due to computational and methodological complexities, that potential remains unmet. This paper attempts to fill this void, combining spatial and spatio-temporal processes, matrix factorization techniques, and hierarchical regression models with player tracking data to advance the state of defensive analytics in the NBA. Our approach detects, characterizes, and quantifies multiple aspects of defensive play in basketball, supporting some common understandings of defensive effectiveness, challenging others, and opening up many new insights into the defensive elements of basketball.

*The authors would like to thank STATS LLC for providing us with the optical tracking data, as well as Ryan Adams, Edo Airolidi, Dan Cervone, Alex D'Amour, Carl Morris, and Natesh Pillai for numerous valuable discussions.

Contents

1	Introduction	2
1.1	Method Overview	3
2	Who’s Guarding Whom	4
2.1	Inference	6
2.2	Results	7
3	Parameterizing Shot Types	9
3.1	Point Process Decomposition	9
3.2	Fitting the LGCPs	11
3.3	NMF Optimization	13
3.4	Basis and Player Summaries	13
4	Frequency and Efficiency: Characteristics of a Shooter	15
4.1	Shrinkage and Parameter Regularization	15
4.2	Shot Frequency	17
4.3	Shot Efficiency	18
4.4	Inference	20
5	Results	21
6	Discussion	24
	References	26

1. Introduction

In contrast to American football, where different sets of players compete on offense and defense, in basketball every player must play both roles. Thus, traditional ‘back of the baseball card’ metrics which focus on offensive play are inadequate for fully characterizing player ability. Specifically, the traditional box score includes points, assists, rebounds, steals and blocks per game, as well as season averages such as field goal percentage and free throw percentage. These statistics paint a more complete picture of the *offensive* production of a player, while steals, blocks, and defensive rebounds provide only a limited summary of *defensive* effectiveness. These metrics, though they explain only a small fraction of defensive play, persist because they summarize recognizable events that are straightforward to record.

A deeper understanding of defensive skill requires that we move beyond simple observables. Due to the inefficacy of traditional defensive statistics, modern understanding of defensive skill has centered around expert intuition and analysis that can be prone to human biases and imprecision. In general, there has been little research characterizing individual player habits in dynamic, goal-based sports such as basketball. This is due to 1) the lack of relevant data, 2) the unique spatial-temporal nature of the sport and 3) challenges associated with disentangling confounded player effects.

One of the most popular metrics for assessing player ability, individual plus/minus, integrates out the details of play, focusing instead on aggregate outcomes. Specifically, this statistic measures the total team point or goal differential while a player is in the game. As such, it represents a notion of overall skill that incorporates both offensive and defensive ability. The biggest difficulty with individual plus/minus, however, is player confounding. That is, plus/minus depends crucially on the skill of an individual’s teammates. One solution to this problem is to aggregate the data further by recording empirical plus/minus for all pairs or even triplets of players in the game (Kubatko et al., 2007). As an alternative, several approaches control for confounding using regression adjusted methods (Rosenbaum, 2004; Sill, 2010; Macdonald, 2011).

Only recently have more advanced hierarchical models been used to analyze individual player ability in sports. In hockey, for instance, competing process hazard models have been used to value players, whereby outcomes are goals, with censoring occurring at each player change (Thomas et al., 2013). As with all of the plus/minus approaches discussed earlier, this analysis looked at discrete outcomes, without taking into consideration within-possession events such as movements, passes, and spatial play formations. Specifically, without analyzing the spatial actions occurring within a possession, measuring individual traits as separate from team characteristics is fraught with identifiability problems.

There is an emerging solution to these identifiability concerns, however, as player tracking systems become increasingly prevalent in professional sports arenas. For this research, we use optical player tracking data from the 2013-2014 NBA season through February 7, 2014. The data, which is derived from cameras mounted in stadium rafters, consist primarily of x, y coordinates for the

ball and all ten athletes on the court (five on each team), recorded at 25 frames per second. In addition, the data include game and player specific annotations: who possesses the ball, when fouls occur, and shot outcomes.

This data enables us for the first time to use spatial and spatio-temporal information to solve some of the challenges associated with individual player analysis. Specifically, the spatial resolution of these data have changed the types of questions we can answer about the game, allowing for in-depth analyses into individual players (Goldsberry, 2012, 2013). Model-based approaches using this rich data have also recently gained traction, with Cervone et al. (2014) employing multi-scale semi-Markov models to conduct real-time evaluations of basketball plays.

While it is clear that player tracking systems have the potential to enable a richer quantitative characterization of basketball performance, this potential has not yet been met, particularly for measuring defensive performance. Rather than integrate out the details of play, we exploit the spatio-temporal information in the data to learn the circumstances that lead to a particular outcome. In this way, we infer not just who benefits their team, but *why* and *how* they do so. Specifically, we develop a model of the spatial behavior of NBA basketball players which reveals interpretable dimensions of both offensive and defensive efficacy.

1.1. Method Overview

We seek to fill a void in basketball analytics by providing the first quantitative characterization of man-to-man defensive effectiveness in different regions of the court. To this end, we propose a model which explains both shot selection (who shoots and where) as well as the expected outcome of the shot, given the defensive assignments. We term these quantities shot *frequency* and *efficiency*, respectively. Despite the abundance of data, critical information for determining these defensive habits is unavailable. First and most importantly, the defensive matchups are unknown. While it is often clear to a human observer who is guarding whom, such information is absent from the data. Secondly, in order to provide meaningful spatial summaries of player ability, we must define relevant court regions in a data driven way. Thus, before we can begin modeling defensive ability, we devise methods to learn these features from the available data.

To accomplish the first task of learning who is guarding whom, we build a model to infer defensive intent over the course of a possession. Specifically, we model man-to-man defense using a variant of the hidden Markov model. From this, we record the amount of time each defensive player spends guarding every offensive player throughout the possession and which defender is guarding the shooter at the moment the shot is taken.

For the second task we find a ‘soft partition’ of the court using a point process decomposition blending log Gaussian Cox processes with non-negative matrix factorization. This affords a data driven, low-dimensional representation of the court. While this court discretization improves computational tractability, it also provides an intuitive way to describe *spatial* variations in player skill.

Given this new information, we are able to model the outcome of each possession by jointly parameterizing the spatial habits and skill of each offensive player as well as the spatial skill of each defensive player. Our results are largely consistent with commonly held beliefs about the adroitness of individual players. For instance, Chris Paul, the 2013-2014 league leader in steals, reduces shot attempts nearly everywhere on the court, relative to similar defenders. However, using inferred defensive matchups, we are the first, to our knowledge, to provide quantitative answers to detailed questions like “How often does Chris Paul let his man get to the basket for a shot attempt?”

Our results reveal other details of play that are not readily apparent. As one example, we demonstrate that two highly regarded defensive centers, Roy Hibbert and Dwight Howard, impact the game in opposing ways. Hibbert reduces shot efficiency near the basket more than any other player in the game, but also faces more shots there than similar players. Howard, on the other hand, is one of the best at reducing shot frequency in this area, but is worse than average at reducing shot efficiency. We synthesize the spatially varying efficiency and frequency results visually in the *defensive* shot chart, a new analogue to the oft depicted offensive shot chart.

2. Who’s Guarding Whom

For each possession, before modeling defensive skill, we must establish some notion of defensive intent. To this end, we first construct a model to identify which offender is guarded by each defender at every moment in time. To identify who’s guarding whom, we infer the canonical position for a defender guarding a particular offender at every time t as a function of space-time covariates. A player deviates from this position due to player or team specific tendencies and unmodeled covariates. Throughout each possession, we index each defensive player by $j \in 1, \dots, 5$ and each offensive player by $k \in 1, \dots, 5$. Without loss of generality, we transform the space so that all possessions occur in the same half. To start, we model the canonical defensive location for a defender at time t , guarding offender k , as a convex combination of three locations: the position of the offender, O_{tk} , the current location of the ball, B_t , and the location of the hoop, H . Let μ_{tk} be the canonical location for a defender guarding player k at time t . Then,

$$\begin{aligned}\mu_{tk} &= \gamma_o O_{tk} + \gamma_b B_t + \gamma_h H \\ \Gamma \mathbf{1} &= \mathbf{1}\end{aligned}$$

with $\Gamma = [\gamma_o, \gamma_b, \gamma_h]$.

Let I_{tjk} be an indicator for whether defender j is guarding offender k at time t . Multiple defenders can guard the same offender, but each defender can only be guarding one offender at any instant. The observed location of a defender j , given that they are guarding offender k , is normally distributed about the mean location

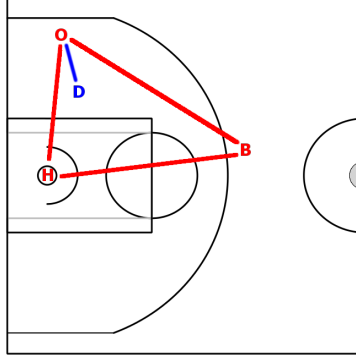


FIG 1. The canonical defending location is a convex combination of the offender, ball and hoop locations.

$$D_{tj}|I_{tjk} = 1 \sim N(\mu_{tk}, \sigma_D^2)$$

We model the evolution of man-to-man defense (as given by the matrix of matchups, \mathbf{I}) over the course of a possession using a hidden Markov model. The hidden states represent the offender that is being guarded by each defensive player. The complete data likelihood is

$$\begin{aligned} L(\Gamma, \sigma_D^2) &= P(\mathbf{D}, \mathbf{I} | \Gamma, \sigma_D^2) \\ &= \prod_{t,j,k} [P(D_{tj}|I_{tjk}, \Gamma, \sigma_D^2) P(I_{tjk}|I_{(t-1)j.})]^{I_{tjk}} \end{aligned}$$

where $P(D_{tj}|I_{tjk} = 1, \Gamma, \sigma_D^2)$ is a normal density as stated above. We also assume a constant transition probability, i.e. a defender is equally likely, a priori, to switch to guarding any offender at every instant

$$\begin{aligned} P(I_{tjk} = I_{(t-1)jk}) &= \rho \\ P(I_{tjk} = I_{(t-1)jk'}) &= \frac{1-\rho}{4}, \quad k' \neq k \end{aligned}$$

for all defenders, j . In this application we fix $\rho = 0.99$ which, given the average number of 200 data points per possession, corresponds to an 86% a priori chance of at least one defensive switch during a possession. The complete

log likelihood is

$$\begin{aligned}
\ell(\Gamma, \sigma_D^2) &= \log P(\mathbf{D}, \mathbf{I} | \Gamma, \sigma_D^2) \\
&= \sum_{t,j,k} I_{tjk} [\log(P(D_{tj} | I_{tjk}, \Gamma, \sigma_D^2)) + \log(P(I_{tjk} | I_{(t-1)j}))] \\
&= \sum_{t,j,k} \frac{I_{tjk}}{\sigma_D^2} (D_{tj} - \mu_{tk})^2 + I_{tjk} \log P(I_{tjk} | I_{(t-1)j})
\end{aligned}$$

2.1. Inference

We use the EM algorithm to estimate the relevant unknowns, I_{tjk} , σ_D^2 , and Γ . At each iteration, i , of the algorithm, we perform the E-step and M-step until convergence. In the E-step, we compute $E_{tjk}^{(i)} = E[I_{tjk} | D_{tj}, \hat{\Gamma}^{(i)}, \hat{\sigma}_D^{2(i)}]$ for all t , j and k . These expectations can be computed using the forward-backward algorithm. Since we assume each defender acts independently, we run the forward-backward algorithm for each j , to compute the expected assignments for each defender. In the M-step, we update the maximum likelihood estimates of σ_D^2 and Γ given the current expectations, $E_{tjk}^{(i)}$, for all t and k .

Let $\mathbf{X} = [\mathbf{O}, \mathbf{B}, \mathbf{H}]$ be the design matrix corresponding to the offensive location, ball location and hoop location. We define $X_{tk} = [O_{tk}, B_t, H]$ to be the row of the design matrix corresponding to offender k at time t .

In the i th iteration of the M-step we update our estimates

$$(\hat{\Gamma}^{(i)}, \hat{\sigma}_D^{2(i)}) \leftarrow \arg \max_{\Gamma, \sigma_D^2} \sum_{t,j,k} \frac{E_{tjk}^{(i-1)}}{\sigma_D^2} (D_{tj} - \Gamma X_{tk})^2, \quad \Gamma \mathbf{1} = 1$$

This maximization corresponds to the solution of a constrained generalized least squares problem and can be found analytically. Let Ω be the diagonal matrix of weights, in this case whose entries at each iteration are $\sigma_D^2 / E_{tjk}^{(i)}$. As $\hat{\Gamma}$ is the maximum likelihood estimator subject to the constraint that $\hat{\Gamma} \mathbf{1} = 1$, it can be shown that

$$\hat{\Gamma} = \hat{\Gamma}_{gls} + (X^T \Omega^{-1} X)^{-1} \mathbf{1}^T (\mathbf{1} (X^T \Omega^{-1} X)^{-1} \mathbf{1}^T)^{-1} (1 - \hat{\Gamma}_{gls} \mathbf{1}),$$

where, $\hat{\Gamma}_{gls} = (X^T \Omega^{-1} X)^{-1} X^T \Omega^{-1} D$ is the usual generalized least squares estimator. Finally, the estimated defender variation at iteration i , $\hat{\sigma}_D^2$, is simply:

$$\hat{\sigma}_D^2 = \frac{(D - \hat{\Gamma} X)^T \mathcal{E} (D - \hat{\Gamma} X)}{N_X}$$

Where $\mathcal{E} = \text{diag}(E_{tjk}^{(i-1)})$ for all t, j, k in iteration i and $N_X = \text{nrow}(X)$. Using these equations, we iterate until convergence, saving the final estimates of $\hat{\Gamma}$ and $\hat{\sigma}_D^2$.

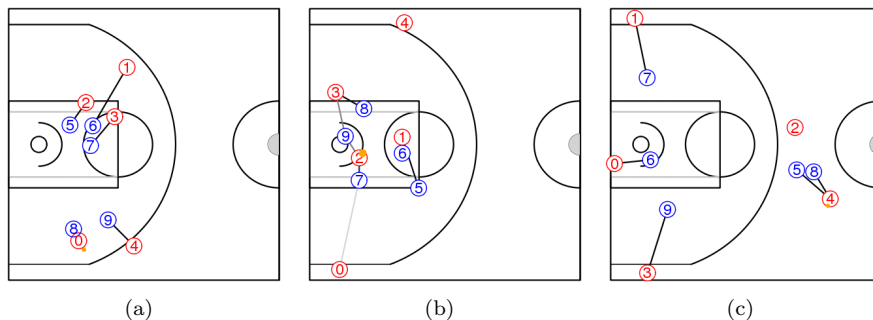


FIG 2. *Who's guarding whom.* Players 0-4 (red) are the offenders and players 5-9 (blue) are defense. Line darkness represents degree of certainty. We illustrate a few properties of the model: (a) Defensive assignments are not just about proximity—defender 6 is closer to offenders 2 and 3, but is in fact guarding player 1. (b) There is more uncertainty about who is guarding who near the basket. (c) Our model captures double teams (defenders 5 and 8 guarding 4).

2.2. Results

First, we restrict our analysis to the parts of a possession in which all players are in the offensive half court – when the ball is moved up the court at the beginning of each possession, most defenders are not yet actively guarding an offender. We use the EM algorithm to fit the HMM on 30 random possessions from the database. We find that a defender's canonical position can be described as $0.62O_t + 0.11B_t + 0.27H$ at any moment in time. That is, we infer that on average the defenders position themselves roughly two thirds of the way between the hoop and the offender they are guarding, shading slightly toward the ball (see Figure 1). Since the weights are defined on a relative, rather than absolute scale, the model implies that defenders guard players more closely when they are near the basket. Furthermore, the model captures the fact that a defender guards the ball carrier more closely, since the ball and the offender are in roughly the same position. In this case, on average the defender positions himself roughly three fourths of the way between the ball carrier and the basket.

As a sensitivity analysis, we fit EM in 100 different games, on different teams, using only 30 possessions for estimating the parameters of the model. The results show that thirty possessions are enough to learn the weights to reasonable precision and that they are stable across games: $\hat{\Gamma} = (0.62 \pm 0.02, 0.11 \pm 0.01, 0.27 \pm 0.02)$. Empirically, the algorithm does a good job of capturing who's guarding whom. Figure 2 illustrates a few snapshots from the model. While there is often some uncertainty about who's guarding whom near the basket, the model accurately infers switches and double teams.

This model is clearly interesting in its own right, but most importantly it facilitates a plethora of new analyses which incorporate matchup defense. For instance, the model could be used to improve *counterpart statistics*, a measure

of how well a player’s counterpart performs (Kubatko et al., 2007). Our model circumvents the challenges associated with identifying the most appropriate counterpart for a player, since we directly infer who is guarding whom at every instant of a possession.

The model can also be used to identify how much defensive attention each offender receives. Table 1 shows the league leaders in attention received, when possessing the ball and when not possessing the ball. We calculate the average attention each player receives as the total amount of time guarded by all defenders divided by the total time playing. This metric reflects the perceived threat of different offenders. The measure also provides a quantitative summary of exactly how much a superstar may free up other shooters on his team, by drawing attention away from them.

On Ball			Off Ball		
Rank	Player	Attention	Rank	Player	Attention
1	DeMar DeRozan	1.215	1	Derrick Rose	1.063
2	Kevin Durant	1.212	2	Stephen Curry	1.059
3	Rudy Gay	1.209	3	Rudy Gobert	1.058
4	Ramon Sessions	1.192	4	Kevin Durant	1.055
5	Joe Johnson	1.190	5	Carmelo Anthony	1.051

TABLE 1

Average attention drawn, on and off ball. Using inference about who’s guarding whom, we calculate the average attention each player receives as the total amount of time guarded by each defender divided by the total time playing (subset by time with and without the ball).

At any moment in time, there are five defenders, and hence five units of “attention” to divide amongst the five offenders each possession. On ball, the players receiving the most attention are double teamed an average of 20% of their time possessing the ball. Off ball, the players that command the most attention consist of MVP caliber players as well as the rookie, Rudy Gobert, who at 7’2 is one of the tallest players currently in the game.

Alternatively, we can define some measure of *defensive entropy*: the uncertainty associated with whom a defender is guarding throughout a possession. This may be a useful notion, since it reflects how active a defender is on the court, in terms of switches and double teams. If each defender guards only a single player throughout the course of a possession, the defensive entropy is zero. If they split their time equally between two offenders, their entropy is one. Within a possession, we define a defender’s entropy as $\sum_{k=1}^5 Z_n(j, k) \log(Z_n(j, k))$, where $Z_n(j, k)$ is the fraction of time defender j spends guarding offender k in possession n .

By averaging defender entropy over all players on a defense, we get a simple summary of a team’s tendency for defensive switches and double teams. Table 2 shows average team entropies, averaged over all defenders within a defense as well as a separate measure averaging over all defenders faced by an offense (induced entropy). By this measure, the Miami Heat are the most active team defense, and additionally they induce the most defensive entropy as an offense.

These results illustrate the many types of analyses that can be conducted. However, in this paper we emphasize the use of matchup defense for inferring individual spatially referenced defender skill. Using information about how long defenders guard offenders and who they are guarding at the moment of the shot,

Rank	Team	Entropy	Rank	Team	Induced Entropy
1	Mia	0.574	1	Mia	0.535
2	Phi	0.568	2	Dal	0.526
3	Mil	0.543	3	Was	0.526
4	Bkn	0.538	4	Chi	0.524
5	Tor	0.532	5	LAC	0.522
26	Cha	0.433	26	OKC	0.440
27	Chi	0.433	27	NY	0.440
28	Uta	0.426	28	Min	0.431
29	SA	0.398	29	Phi	0.428
30	Por	0.395	30	LAL	0.418

TABLE 2

Team defensive entropy. A player's defensive entropy for a particular possession is defined as $\sum_{k=1}^5 Z_n(j, k) \log(Z_n(j, k))$, where $Z_n(j, k)$ is the fraction of time the defender j spends guarding offender k during possession n . Team defensive entropy is defined as the average player entropy over all defensive possessions for that team. Induced entropy is the average player entropy over all defenders facing a particular offense.

we can estimate how defenders affect both shot selection and shot efficiency in different parts of the court. Still, given the high resolution of the spatial data and relatively low sample size per player, inference is challenging. As such, before proceeding we find an interpretable, data driven, low-dimensional spatial representation of the court on which to estimate these defender effects.

3. Parameterizing Shot Types

In order to concisely represent players' spatial offensive and defensive ability, we develop a method to find a succinct representation of the court by using the locations of attempted shots. Shot selection in professional basketball is highly structured. We leverage this structure by finding a low dimensional decomposition of the court whose components intuitively corresponds to *shot type*. A *shot type* defines a spatially smooth intensity surface over the court that indicates where that shot type tends to come from (and where it does not come from). Each player's shooting habits are then represented by a positive linear combination of the global shot types.

Defining a set of global shot types shared among players is beneficial for multiple reasons. Firstly, it allows us to concisely parameterize spatial phenomena with respect to shot type (for instance, the ability of a defensive player to contest a corner three point shot). Secondly, it provides a low dimensional representation of player habits that can be used to specify a prior on both offensive and defensive parameters for possession outcomes. The graphical and numerical results of this model can be found in Section 3.4.

3.1. Point Process Decomposition

Our goal is to simultaneously identify a small set of \mathcal{B} global *shot types* and each player's loadings onto these shot types. We accomplish this with a two-step procedure. First, we find a nonparametric estimate of each player's smooth intensity

surface, modeled as a log Gaussian Cox process (LGCP) (Møller et al., 1998). Second, we find an optimal low rank representation of all players' intensity surfaces using non-negative matrix factorization (NMF) (Lee and Seung, 1999). The LGCP incorporates individual spatial information about shots while NMF pools together global information across players. This pooling smooths each player's estimated intensity surface and yields more robust generalization. For instance, for $\mathcal{B} = 6$, the average predictive ability across players of LGCP+NMF outperforms the predictive ability of independent LGCP surfaces on out of sample data. Intuitively, the global bases define long range correlations that are difficult to capture with a stationary covariance function.

We model a player's shot attempts as a point process on the offensive half court, a 47 ft by 50 ft rectangle. Again, shooters will be indexed by $k \in \{1, \dots, K\}$, and the set of each player's shot attempts will be referred to as $\mathbf{x}_k = \{x_{k,1}, \dots, x_{k,N_k}\}$, where N_k is the number of shots taken by player k , and $x_{k,m} \in [0, 47] \times [0, 50]$.

Though we have formulated a continuous model for conceptual simplicity, we discretize the court into V one-square-foot tiles for computational tractability of LGCP inference. We expect this tile size to capture all interesting spatial variation. Furthermore, the discretization maps each player into \mathbb{R}_+^V , which is necessary for the NMF dimensionality reduction.

Given point process realizations for each of K players, $\mathbf{x}_1, \dots, \mathbf{x}_K$, our procedure is

1. Construct the count matrix \mathbf{X}_{kv} = number of shots by player k in tile v on a discretized court.
2. Fit an intensity surface $\lambda_k = (\lambda_{k1}, \dots, \lambda_{kV})^T$ for each player k over the discretized court (LGCP) (Figure 3(b)).
3. Construct the data matrix $\mathbf{\Lambda} = (\bar{\lambda}_1, \dots, \bar{\lambda}_K)^T$, where $\bar{\lambda}_k$ has been normalized to have unit volume.
4. Find low-rank matrices \mathbf{L}, \mathbf{W} such that $\mathbf{WL} \approx \mathbf{\Lambda}$, constraining all matrices to be non-negative (NMF) (Figure 3(c)).

This procedure yields a spatial basis \mathbf{L} and basis loadings, $\hat{\mathbf{w}}_k$, for each individual player.

One useful property of the Poisson process is the superposition theorem (Kingman, 1992), which states that given a countable collection of independent Poisson processes $\mathbf{x}_1, \mathbf{x}_2, \dots$, each with intensity $\lambda_1, \lambda_2, \dots$, their superposition is distributed as

$$\bigcup_{i=1}^{\infty} \mathbf{x}_i \sim \mathcal{PP} \left(\sum_{i=1}^{\infty} \lambda_i \right).$$

Consequently, with the non-negativity of the basis and loadings from the NMF procedure, the basis vectors can be interpreted as sub-intensity functions, or 'shot types', which are archetypal intensities used by each player. The linear weights for each player concisely summarize the spatial shooting habits of a player into a vector in $\mathbb{R}_+^{\mathcal{B}}$.

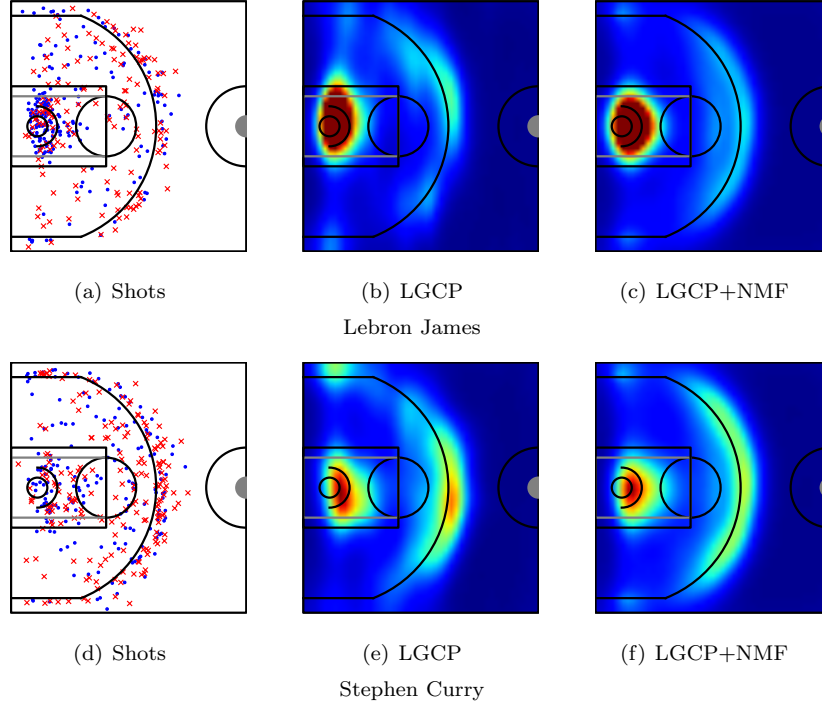


FIG 3. *NBA player shooting representations, from left to right: original point process data from two players, LGCP surface, and NMF reconstructed surfaces ($B = 6$). Made and missed shots are represented as blue circles and red \times 's, respectively.*

3.2. Fitting the LGCPs

For each player's set of points, \mathbf{x}_k , the likelihood of the point process is discretely approximated as

$$p(\mathbf{x}_k | \lambda_k(\cdot)) \approx \prod_{v=1}^V p_{\text{pois}}(\mathbf{X}_{kv} | \Delta A \lambda_{kv})$$

where, overloading notation, $\lambda_k(\cdot)$ is the exact intensity function, λ_k is the discretized intensity function (vector), ΔA is the area of each tile (implicitly one from now on), and $p_{\text{pois}}(\cdot | \lambda)$ is the Poisson probability density function with mean λ . This approximation comes from the completely spatially random property of the Poisson process, which renders disjoint subsets of space independent. Formally, for two disjoint subsets $A, B \subset \mathcal{X}$, after conditioning on the intensity the number of points that land in each set, N_A and N_B , are independent. Under the discretized approximation, the probability of the number of shots in each tile is Poisson, with uniform intensity λ_{kv} .

Explicitly representing the Gaussian random field \mathbf{z}_k , the posterior is

$$\begin{aligned} p(\mathbf{z}_k | \mathbf{x}_k) &\propto p(\mathbf{x}_k | \mathbf{z}_k) p(\mathbf{z}_k) \\ &= \prod_{v=1}^V e^{-\lambda_{kv}} \frac{\lambda_{kv}^{\mathbf{x}_{kv}}}{\mathbf{x}_{kv}!} \mathcal{N}(\mathbf{z}_k | 0, \mathbf{C}) \\ \lambda_n &= \exp(\mathbf{z}_k + z_0) \end{aligned}$$

where the prior over \mathbf{z}_k is a mean zero normal with covariance

$$\mathbf{C}_{vu} \equiv c(\mathbf{x}_v, \mathbf{x}_u) = \sigma^2 \exp \left(-\frac{1}{2} \sum_{d=1}^2 \frac{(x_{vd} - x_{ud})^2}{\nu_d^2} \right)$$

and z_0 is an intercept term that parameterizes the mean rate of the Poisson process. This kernel is chosen to encode prior belief in the spatial smoothness of player habits. Furthermore, we place a gamma prior over the length scale, ν_k , for each individual player. This gamma prior places mass dispersed around 8 feet, indicating the reasonable a priori belief that shooting variation is locally smooth on that scale. Note that $\nu_k = (\nu_{k1}, \nu_{k2})$, corresponding to the two dimensions of the court. We obtain posterior samples of λ_k and ν_k by iteratively sampling $\lambda_k | \mathbf{x}_k, \nu_k$ and $\nu_k | \lambda_k, \mathbf{x}_k$.

We use Metropolis-Hastings to generate samples of $\nu_k | \lambda_k, \mathbf{x}_k$. Naively computing the likelihood term necessitates inverting the spatial covariance, an $O(V^3)$ operation (where $V = 47 \times 50 = 2350$, the number of tiles on the grid). At every sampling iteration, computing this inverse would be prohibitively expensive. However, because the covariance function factors across the two dimensions and we are only considering the covariances between points on a fixed grid, the covariance matrix $\text{cov}(\mathbf{z}_k) \equiv \mathbf{C}$ can be expressed as the Kronecker product of two smaller matrices

$$\mathbf{C} = \mathbf{C}_1 \otimes \mathbf{C}_2$$

where $(\mathbf{C}_1)_{vu}$ is the covariance matrix along the first dimension of the court (along the sideline), and

$$(\mathbf{C}_1)_{vu} = \sigma \exp \left(-\frac{1}{2} \frac{(x_{v1} - x_{u1})^2}{\nu_1^2} \right) \quad (3.1)$$

for $uv \in \{1, \dots, 47\}$. Similarly, $(\mathbf{C}_2)_{vu}$ is the covariance matrix along the second dimension of the court (along the baseline). The inverse of the Kronecker product of two matrices is the Kronecker product of the inverses, which makes inverting \mathbf{C} an $O(V^{3/2})$ operation, which dramatically speeds up computation (Saatchi, 2011). Furthermore, we ‘whiten’ the latent field according to Algorithm 2 in Murray and Adams (2010) to accelerate mixing.

Samples of the latent intensity surface, $\lambda_k | \mathbf{x}_k, \nu_k$ are generated by transforming samples of $\mathbf{z}_k, \nu_k | \mathbf{x}_k$. To overcome the high correlation induced by the court’s spatial structure, we employ elliptical slice sampling (Murray et al., 2010), and subsequently store the posterior mean. Elliptical slice sampling requires a Cholesky decomposition, which can be computed in $O(V^{3/2})$ by again exploiting the Kronecker structure of \mathbf{C} and Algorithm 15 in Saatchi (2011).

3.3. NMF Optimization

Identifying non-negative linear combinations of global shot types can be directly mapped to non-negative matrix factorization. NMF assumes that some matrix $\mathbf{\Lambda}$, in our case the matrix of player-specific intensity functions, can be approximated by the product of two low rank matrices

$$\mathbf{\Lambda} = \mathbf{W}\mathbf{L}$$

where $\mathbf{\Lambda} \in \mathbb{R}_+^{N \times V}$, $\mathbf{W} \in \mathbb{R}_+^{N \times \mathcal{B}}$, and $\mathbf{L} \in \mathbb{R}_+^{\mathcal{B} \times V}$, and we assume $\mathcal{B} \ll V$. The optimal matrices \mathbf{W}^* and \mathbf{L}^* are determined by an optimization procedure that minimizes $\ell(\cdot, \cdot)$, a measure of reconstruction error or divergence between $\mathbf{W}\mathbf{L}$ and $\mathbf{\Lambda}$ with the constraint that all elements remain non-negative

$$\mathbf{W}^*, \mathbf{L}^* = \arg \min_{\mathbf{W}_{ij}, \mathbf{L}_{ij} \geq 0} \ell(\mathbf{\Lambda}, \mathbf{W}\mathbf{L}).$$

Different choices of ℓ will result in different matrix factorizations. A natural choice is the matrix divergence metric

$$\ell_{\text{KL}}(\mathbf{X}, \mathbf{Y}) = \sum_{i,j} X_{ij} \log \frac{X_{ij}}{Y_{ij}} - X_{ij} + Y_{ij}$$

which corresponds to the Kullback-Leibler (KL) divergence if \mathbf{X} and \mathbf{Y} are discrete distributions, i.e., $\sum_{i,j} X_{ij} = \sum_{i,j} Y_{ij} = 1$ (Lee and Seung, 2001). Although there are several other possible divergence metrics (i.e. Frobenius), we use this KL-based divergence measure for reasons outlined in Miller et al. (2014). We solve the optimization problem using techniques from Lee and Seung (2001) and Brunet et al. (2004).

Due to the positivity constraint, the basis \mathbf{L}^* tends to be disjoint, exhibiting a more ‘parts-based’ decomposition than other, less constrained matrix factorization methods, such as PCA. This is due to the restrictive property of the NMF decomposition that disallows negative bases to cancel out positive bases. In practice, this restriction eliminates a large swath of ‘optimal’ factorizations with negative basis/weight pairs, leaving a sparser and often more interpretable basis (Lee and Seung, 1999).

3.4. Basis and Player Summaries

We graphically depict the shot type preprocessing procedure in Figure 3. A player’s spatial shooting habits are reduced from a raw point process to an independent intensity surface, and finally to a linear combination of \mathcal{B} nonnegative basis surfaces. There is wide variation in shot selection among NBA players - some shooters specialize in certain types of shots, whereas others will shoot from many locations on the court.

Setting $\mathcal{B} = 6$ and using the KL-based loss function, we display the resulting basis vectors in Figure 4. This procedure identifies basis vectors that correspond

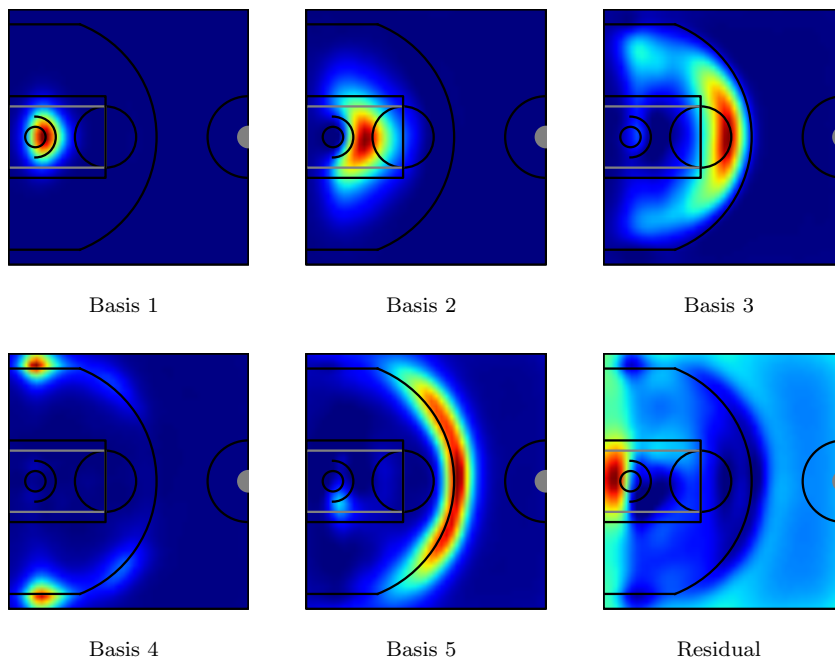


FIG 4. *Basis vectors (surfaces) identified by LGCP-NMF for $\mathcal{B} = 6$. Each basis surface is the normalized intensity function of a particular shot type, and players' shooting habits are a weighted combination of these shot types. Conditioned on a certain shot type (e.g. corner three), the intensity function acts as a density over shot locations, where red indicates likely locations.*

to spatially interpretable shot types. Similar to the parts-based decomposition of human faces that NMF yields in [Lee and Seung \(1999\)](#), LGCP-NMF yields a shots-based decomposition of NBA players. For instance, it is clear from inspection that one basis corresponds to shots in the restricted area, while another corresponds to shots from the rest of the paint. The three point line is also split into corner three point shots and center three point shots. Unlike PCA, NMF is not mean-centered, and as such a residual basis appears regardless of \mathcal{B} ; this basis in effect captures positive intensities outside of the support of the relevant bases. In all analyses herein, we discard the residual basis and work solely with the remaining bases.

The LGCP-NMF decomposition also yields player specific shot weights that provide a concise characterization of their offensive habits. The weight w_{kb} can be interpreted as the amount player k takes shot type b , which quantifies intuitions about player behavior. [Table 5](#) compares normalized weights between a selection of players. While these weights summarize offensive *habits*, our aim is to develop a model to jointly measure both offensive and defensive *ability* in different parts of the court. Using who's guarding whom and this data driven court discretization, we proceed by developing a model to quantify the effect

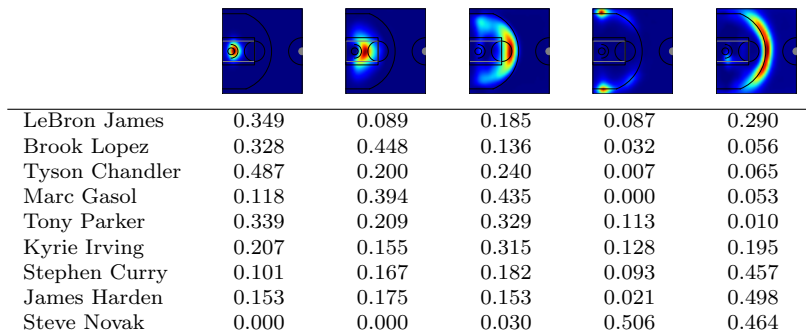


FIG 5. Normalized player weights for each basis. The first two columns correspond to close-range shots, the third column to mid-range shots, and the last two to three-point shots. The weights themselves match intuition about players shooting habits (e.g. three-point specialist or mid-range shooter), while more exactly quantifying them.

that defenders have on both shot selection (frequency) and shot efficiency.

4. Frequency and Efficiency: Characteristics of a Shooter

We proceed by decomposing a player’s habits in terms of shot frequency and efficiency. First, we construct a model for where on the court different offenders prefer to shoot. This notion is often portrayed graphically as the *shot chart* and reflects a player’s spatial shot *frequency*. Second, conditioned on a player taking a shot, we want to know the probability that the player actually makes the shot: the spatial player *efficiency*. Together, player spatial shot *frequency* and *efficiency* largely characterize a basketball player’s habits and ability.

While it is not difficult to empirically characterize frequency and efficiency of shooters, it is much harder to say something about how defenders affect these two characteristics. Given knowledge of matchup defense, however, we can create a more sophisticated joint model which incorporates how defenders affect shooter characteristics. Using the results on who’s guarding whom, we are able to provide estimates of defensive impact on shot frequency and efficiency, and ultimately a defensive analogue to the offensive shot chart (Figure 3(a)).

4.1. Shrinkage and Parameter Regularization

Parameter regularization is a very important part of our model because many players are only observed in a handful of plays. We shrink estimates by exploiting the notion that players with similar roles should be more similar in their capabilities. However, because offense and defense are inherently different, we must characterize player similarity separately for offense and defense.

First, we gauge how much variability there is between defender types. One measure of defender characteristics is the fraction of time, on average, that each defender spends guarding a shooter in each of the \mathcal{B} bases. Figure 6 suggests

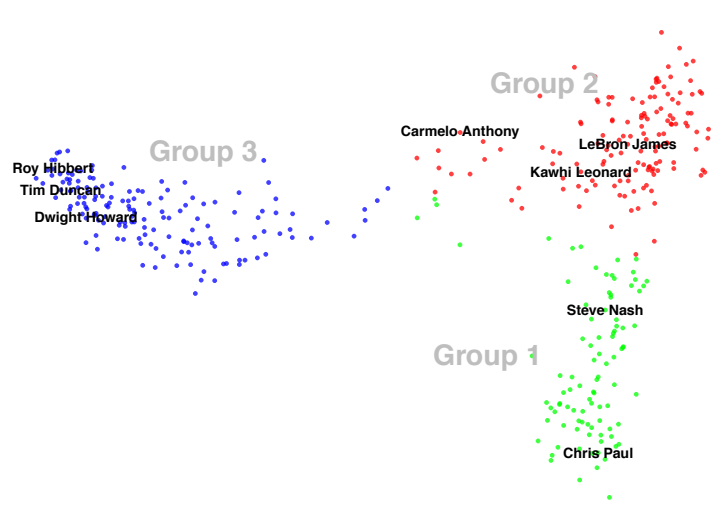


FIG 6. *Defensive Clusters.* We ran SVD on the $N \times \mathcal{B}$ matrix of time spent in each basis. The first two principle components suggest that three clusters reasonably separate player groups. Group 1 (green) roughly corresponds to small point guards, group 2 (red) to forwards and guards, and group 3 (blue) to centers.

that defenders can be grouped into roughly three defender types. The groupings are inferred using three cluster K-means on the first two principle component vectors of the “time spent” matrix. Empirically, group 1 corresponds to small point guards, group 2 to forwards and guards, and group 3 to centers. We use these three groups to define the shrinkage points for defender effects in both the shot selection and shot efficiency models.

When we repeat the same process for offense, it is clear that the players do not cluster; specifically, there appears to be far more variability in offender types than defender types. Thus, to characterize offender similarity, we instead use the normalized player weights from the non-negative matrix factorization (Figure 5). Figure 7 shows the loadings on the first two principle components of the player weights. The points are colored by the player’s listed position (e.g. guard, center, forward, etc). While players tend to be more similar to players with the same listed position, on the whole, position is not a good predictor of an offender’s shooting characteristics.

Consequently, for the prior distribution on offender efficiency we use a normal conditional autoregressive (CAR) model (Cressie, 1993). For every player, we identify the 10 nearest neighbors in the space of shot selection weights. We then connect two players if, for either player in the pair, their partner is one of their ten closest neighbors. We use this network to define a Gaussian Markov random field prior on offender efficiency effects (Section 4.3).

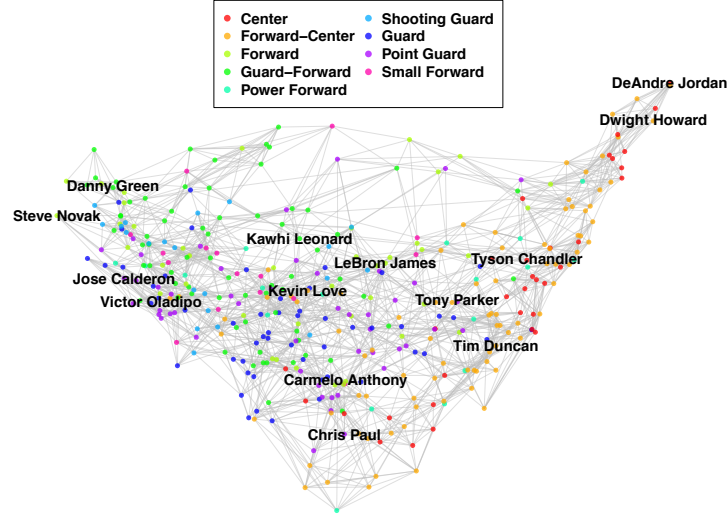


FIG 7. *Offender similarity network.* We ran SVD on the $N \times \mathcal{B}$ matrix of NMF coefficients (Section 3). The projection into the first two principle components shows that there is no obvious clustering of offensive player types, as was the case with defense. Moreover “player position” is not a good indicator of shot selection.

4.2. Shot Frequency

We model shot selection (both shooter and location) using a multinomial distribution. First, we discretize the court into \mathcal{B} regions using the pre-processed NMF basis vectors (see Section 3) and define the multinomial outcomes as one of the $5 \times \mathcal{B}$ shooter/basis pairs. The court regions from the NMF are naturally disjoint (or nearly so). In this paper, we use the first five bases given in Figure 4. Shot selection is a function of the offensive players on the court, the fraction of possession time that they are guarded by different defenders, and defenders’ skills. Letting \mathcal{S}_n be a categorical random variable indicating the shooter and shot location in possession n ,

$$p(\mathcal{S}_n(k, b) = 1 | \alpha, Z_n) = \frac{\exp\left(\alpha_{kb} + \sum_{j=1}^5 Z_n(j, k) \beta_{jb}\right)}{1 + \sum_{mb} \exp\left(\alpha_{kb} + \sum_{j=1}^5 Z_n(j, k) \beta_{jb}\right)}$$

Here, α_{kb} is the propensity for an offensive player, k , to take a shot from basis b . However, in any given possession, a players’ propensity to shoot is affected by the defense. β_{jb} represents how well a defender, j , suppresses shots in a given basis b , relative to the average defender. These values are modulated by entries in a possession specific covariate matrix Z_n . The value $Z_n(j, k)$ is the

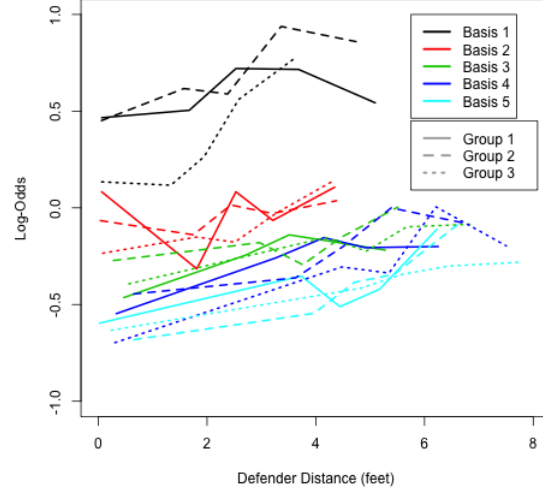


FIG 8. *Shot efficiency vs. distance.* We find plot empirical shot efficiency as a function of the guarding defender’s distance, by region and group (Figure 6). We compute the empirical log-odds of a shot by binning all shots from each region into 5 bins. The log-odds of a made shot appears to be nearly linear in distance, although in some cases this relationship is noisy due to small sample sizes.

fraction of time defender j is guarding offensive player k in possession n , with $\sum_{k=1}^5 Z_n(j, k) = 1$. Note that the baseline outcome is “no shot”, indicating there was a turnover before a shot was attempted.

We assume normal random effects for both the offensive and defensive player parameters:

$$\alpha_{kb} \sim N(\mu_{\alpha b}, \sigma_{\alpha}^2), \quad \beta_{jb} \sim N(\mu_{\beta \mathcal{G} b}, \sigma_{\beta}^2)$$

Here, $\mu_{\alpha b}$ and $\mu_{\beta \mathcal{G} b}$ represent the player average effect in basis b on offense and defense respectively. For defenders, \mathcal{G} indexes one of the 3 defender types (Figure 6), so that there are in fact $3\mathcal{B}$ group means. Finally, we specify that

$$\mu_{\alpha b} \sim N(0, \tau_{\alpha}^2), \quad \mu_{\beta \mathcal{G} b} \sim N(0, \tau_{\beta}^2)$$

4.3. Shot Efficiency

Given a shot, we model efficiency (the probability that the shot is made) as a function of the offensive player’s skill, the defender at the time of the shot, the distance of that defender to the shooter, and where the shot was taken. For a possession n ,

$$p(Y_n = 1 | \mathcal{S}_n(k, b) = 1, j, \mathcal{D}_n, \theta, \phi, \xi) = \frac{\exp(\theta_{kb} + \phi_{jb} + \xi_b \mathcal{D}_n)}{1 + \exp(\theta_{kb} + \phi_{jb} + \xi_b \mathcal{D}_n)}$$

Here, Y_n is an indicator for whether the attempted shot for possession n was made and \mathcal{D}_n is the distance in feet between the shooter and defender at the moment of the shot. The parameter θ_{kb} describes the shooting skill of a player, k , from basis b . Similarly ϕ_{jb} describes the defensive skill of defender j . Within a region, as the defender gets further from the shooter, their effect on the outcome of the shot decreases at the same rate, ξ_b ; as the most likely defender approaches the exact location of the shooter, the defensive effect on the log-odds of a made shot converges toward ϕ_{jb} . Figure 8 supports this modeling choice: empirically, the log-odds of a shot increase roughly linearly in distance. We again employ hierarchical priors to pool information across players. On defense we specify that:

$$\phi_{jb} \sim N(\mu_{\phi \mathcal{G} b}, \sigma_{\phi}^2)$$

Here, $\mu_{\phi \mathcal{G} b}$ represents the player average effect in basis b on defense. Again, \mathcal{G} indexes one of 3 defender types, so that there are in fact $3\mathcal{B}$ group means.

On offense, we use the network defined in Section 4.1 (Figure 7) to specify a CAR prior. We define each player's efficiency to be, a priori, normally distributed with mean proportional to the mean of his neighbors' efficiencies. This operationalizes the notion that players who have more similar shooting habits should have more similar shot efficiencies. Explicitly, the efficiency, θ , of an offender, k in a region b with mean player efficiency $\mu_{\theta b}$ has the prior distribution

$$(\theta_{kb} - \mu_{\theta b}) \sim N\left(\frac{\rho}{|\mathcal{N}(k)|} \sum_{k' \in \mathcal{N}(k)} (\theta_{k'b} - \mu_{\theta b}), \sigma_k^2\right)$$

where $\mathcal{N}(k)$ are the set of neighbors for offender k and $\rho \in [0, 1)$ is a discount factor. These conditionals imply the joint distribution

$$\boldsymbol{\theta}_b \sim N(\boldsymbol{\mu}_{\theta b}, (I - \rho M)^{-1} D)$$

where D is the diagonal matrix with entries $\frac{1}{\sigma_k^2}$ and M is the matrix such that $M_{k,k'} = \frac{1}{|\mathcal{N}(k)|}$ if offenders k and k' are neighbors and zero otherwise. This joint distribution is proper as long as $(I - \rho M)^{-1} D$ is symmetric positive-definite. The matrix is symmetric when $\sigma_k^2 \propto \frac{1}{|\mathcal{N}(k)|}$. We chose $\rho = 0.9$ to guarantee the matrix is positive-definite (Cressie, 1993).

Again we use normal priors for the group means:

$$\mu_{\theta b} \sim N(0, \tau_{\theta}^2), \mu_{\phi b} \sim N(0, \tau_{\phi}^2)$$

Finally, for the distance effect, we specify that

$$\xi_b \sim N^+(0, \tau_\xi^2)$$

where N^+ indicates a half-normal distribution. We chose a prior distribution with positive support, since increased defender distance should logically increase the offenders efficiency.

4.4. Inference

We use Bayesian inference to infer parameters of both the shot frequency and shot efficiency models. First, we consider different methods of inference in the shot frequency model. The sample size, number of categories, and number of parameters in the model for shot selection are all quite large, making full Bayesian inference challenging. Specifically, there are $5 \times \mathcal{B} + 1 = 26$ outcomes (one for each shooter-basis pair plus one for turnovers) and over 70,000 observations. To facilitate computation, we use a local variational inference strategy to approximate the true posterior of parameters from the multinomial logistic regression. The idea behind the variational strategy is to find a lower bound to the multinomial likelihood with a function that looks Gaussian. For notational simplicity let $\boldsymbol{\eta}_n$ be the vector with elements $\eta_{nk} = \alpha_{kb} + \sum_{j=1}^5 Z_n(j, k)\beta_{jb}$. Then, the lower bound takes the form

$$\log P(\mathcal{S}_n | \boldsymbol{\eta}_n) \geq (\mathcal{S}_n + b_n)^T \boldsymbol{\eta}_n - \boldsymbol{\eta}_n^T \mathbf{A} \boldsymbol{\eta}_n - c_n$$

where \mathbf{b}_n and c_n are variational parameters and \mathbf{A} is a simple bound on the Hessian of the log-sum-exp function (Böhning, 1992). This implies a Gaussianized approximation to the observation model. Since we use normal priors on the parameters, this yields a normal approximation to the posterior. By iteratively updating the variational parameters, we maximize the lower bound on the likelihood. This yields the best normal approximation to the posterior in terms of KL-divergence (see Murphy (2012) for details).

In the variational inference, we fix the prior parameters as follows: $\sigma_\alpha^2 = 1$, $\sigma_\beta^2 = 0.01$, $\tau_\alpha^2 = 1$, and $\tau_\beta^2 = 0.01$. That is, we specify more prior variability in the offensive effects than the defensive effects at both the group and individual level. We use cross-validation to select these prior parameters Section 5, where we demonstrate that despite using approximate inference, the model performs well in out of sample prediction. Since the variational method is only approximate, we start with some exploratory analysis to tune the shrinkage hyperparameters. We examine five scales for both the offense and defense group level prior variance to find the shrinkage factors that yield the highest predictive power. Because the random effects are normal and additive, we constrain $\sigma_\beta^2 < \sigma_\alpha^2$ for identifiability. We then fix the sum $\sigma_{total} = \sigma_\alpha^2 + \sigma_\beta^2$, and search over values such that $\sigma_\beta^2 < \sigma_\alpha^2$. We also examine different scales of σ_{total} . This search at multiple values of σ_{total} yields the optimal ratio $\frac{\sigma_\beta^2}{\sigma_\alpha^2}$ to be between 0.1 and 0.2.

For the efficiency model, we found Bayesian logistic regression to be more tractable: in this regression, there are only two outcomes (make or miss) and

	Full Model	No Shrinkage	No Defense	No Spatial
Shooter log-likelihood	-10506.78	-10625.50	-10586.65	-10836.50
Basis log-likelihood	-10589.13	-10683.01	-10636.06	N/A
Full log-likelihood	-17187.96	-17318.45	-17298.19	N/A
Efficiency log-likelihood	-3202.09	-3221.44	-3239.12	-3270.99

TABLE 3

Out of sample log-likelihoods for models of increasing complexity. The first row corresponds to the average out of sample likelihood for predicting only the shooter. The second row similarly summarizes out of sample likelihood for predicting only which basis the shot comes from (not the shooter). The third row is the average out of sample log likelihood over the product space of shooter and shot location. We demonstrate that not only does our model outperform simpler models in predicting possession outcomes, but that we outperform them in both shooter and basis prediction tasks individually. In the fourth row, we display the out of sample likelihoods for shot efficiency (whether the shooter makes the basket). The four different models from left to right are (i) the full offensive and defensive model with parameter shrinkage (incorporating inferred defender type and offender similarity), (ii) the offensive and defensive model with a common shrinkage point for all players, (iii) the offense only model, (iv) the offense only model with no spatial component. Incorporating defensive information, spatial information, and player type clearly yields the best predictive models. All quantities were computed using 10-fold cross validation.

approximately 50,000 possessions which lead to a shot. Thus, we proceed with a fully Bayesian regression on shot efficiency, using the variational inference algorithm to initialize the sampler. Inference in the Bayesian regression for shot efficiency was done using hybrid Monte Carlo (HMC) sampling. We implemented the sampler using the probabilistic programming language STAN ([Stan Development Team, 2014](#)). We use 2000 samples, and ensure that the \hat{R} statistic is close to 1 for all parameters ([Gelman and Rubin, 1992](#)).

5. Results

We fit our model on the data from the first half of the 2013-2014 NBA regular season, focusing on a specific subset of play: possessions lasting at least 3 seconds, in which all players are in the half-court. We also ignore any activity after the first shot and exclude all plays including fouls or stoppages for simplicity.

First, we assess the predictive performance of our model relative to simpler models. For both the frequency and efficiency models, we run ten-fold cross validation and compare four models of varying complexity: (i) the full offense/defense model with defender types and CAR shrinkage, (ii) the full offense/defense model without defender types or CAR shrinkage, (iii) a model that ignores defense completely, (iv) a model that ignores defense and space. The frequency models (i-iii) all include 5 ‘shot-types’, and each possession results in one of 26 outcomes. Frequency model (iv) has only 6 outcomes - who shot the ball (or no shot). The outcomes of the efficiency model are always binary (corresponding to made or missed shots).

Table 3 demonstrates that we outperform simpler models in predicting out of sample shooter-basis outcomes. Moreover, while we do well in joint prediction, we also outperform simpler models for predicting both shooter and shot basis separately. Finally, we show that the full efficiency model also improves upon

simpler models. Consequently, by incorporating spatial variation and defensive information we have created a model that paints a more detailed and accurate picture of the game of basketball.

Basis 1 - Efficiency					
Group 1		Group 2		Group 3	
Player	$\phi + \xi \mathcal{D}^*$	Player	$\phi + \xi \mathcal{D}^*$	Player	$\phi + \xi \mathcal{D}^*$
M. Dellavedova	-0.013	M. Miller	-0.096	R. Hibbert	-0.301
K. Thompson	0.060	T. Hardaway Jr.	-0.075	R. Sacre	-0.265
E. Bledsoe	0.073	K. Singler	-0.063	E. Brand	-0.263
R. Jackson	0.084	P. Pierce	-0.055	A. Horford	-0.245
B. Udrih	0.091	M. Morris	-0.054	V. Faverani	-0.244
<i>Average</i>	0.239	<i>Average</i>	0.080	<i>Average</i>	-0.125
G. Vasquez	0.448	T. Allen	0.326	J. McRoberts	0.018
B. Knight	0.454	J. Smith	0.364	T. Young	0.025
T. Wroten	0.470	E. Gordon	0.386	M. Beasley	0.030
N. Cole	0.486	X. Henry	0.390	C. Boozer	0.054
S. Blake	0.592	M. Thornton	0.476	J. Thompson	0.101

Basis 1 - Frequency					
Group 1		Group 2		Group 3	
Player	β	Player	β	Player	β
C. Paul	-0.448	L. Stephenson	-0.387	L. Aldridge	0.062
T. Parker	-0.444	D. Waiters	-0.377	B. Diaw	0.073
N. Cole	-0.442	J. Crawford	-0.376	N. Pekovic	0.074
J. Nelson	-0.440	M. Webster	-0.361	D. Howard	0.082
G. Hill	-0.439	M. Ginobili	-0.344	L. Scola	0.085
<i>Average</i>	-0.349	<i>Average</i>	-0.258	<i>Average</i>	0.184
P. Mills	-0.260	X. Henry	-0.157	J. Henson	0.286
D. Green	-0.258	J. Smith	-0.152	J. Valanciunas	0.320
S. Marion	-0.256	M. Morris	-0.148	E. Kanter	0.321
G. Dragic	-0.242	D. Wright	-0.148	A. Drummond	0.323
M. Williams	-0.232	A. Shved	-0.134	R. Lopez	0.421

TABLE 4

Basis 1. Shot efficiency (top table) and frequency (bottom table). We list the top and bottom five defenders in terms of the effect on the log-odds on a shooters' shot efficiency in the restricted area (basis 1). Negative effects imply that the defender decreases the log-odds of an outcome, relative to the global average player (zero effect). The three columns consist of defenders in the three groups listed in Figure 6 and the respective group means. Two highly regarded centers, Roy Hibbert and Dwight Howard, are effective in different ways—Hibbert decreases shot efficiency the most of any player, but faces more shots overall, whereas Howard is rated fourth in shot frequency despite a slightly below average effect on efficiency.

As our main results we focus on parameters related to defensive shot selection and shot efficiency effects. Here we focus on defensive results as the novel contribution of this work. A sample of the defensive logistic regression log-odds for basis one (restricted area) and five (center threes) are given in Tables 4 and 5 respectively. For shot selection, we report the defender effects, β_{jb} , which corresponds to the change in log-odds of a shot occurring in a particular region, b , if defender j guards the offender for the entire possession. Smaller values correspond to a reduction in the shooter's shot frequency in that region.

For shot efficiency we report $\phi_j + \xi_b \mathcal{D}_{jb}^*$ where \mathcal{D}_{jb}^* is player j 's difference

Basis 5 - Efficiency					
Group 1		Group 2		Group 3	
Player	$\phi + \xi\mathcal{D}^*$	Player	$\phi + \xi\mathcal{D}^*$	Player	$\phi + \xi\mathcal{D}^*$
S. Blake	-0.184	W. Green	-0.280	S. Battier	-0.085
N. Cole	-0.168	K. Leonard	-0.208	T. Jones	-0.085
A. Bradley	-0.157	L. Stephenson	-0.194	M. Harris	-0.084
S. Larkin	-0.144	T. Prince	-0.190	B. Bass	-0.074
G. Dragic	-0.137	J. Dudley	-0.165	S. Williams	-0.065
<i>Average</i>	-0.052	<i>Average</i>	-0.025	<i>Average</i>	0.043
T. Taylor	0.017	H. Barnes	0.139	A. Blatche	0.186
L. Ridnour	0.025	J. Hamilton	0.181	J. Henson	0.197
D. Morris	0.043	E. Clark	0.190	J. Maxiell	0.198
R. Sessions	0.045	L. Deng	0.204	A. Jefferson	0.267
B. Knight	0.072	D. Waiters	0.205	R. Hibbert	0.344

Basis 5 - Frequency					
Group 1		Group 2		Group 3	
Player	β	Player	β	Player	β
G. Dragic	-0.940	K. Leonard	-0.736	N. Pekovic	-1.174
D. Lillard	-0.934	H. Barnes	-0.695	B. Diaw	-1.165
T. Lawson	-0.922	K. Singler	-0.682	A. Johnson	-1.152
T. Burke	-0.895	A. Afflalo	-0.665	D. Favors	-1.150
M. Williams	-0.877	K. Caldwell-Pope	-0.660	D. Cousins	-1.148
<i>Average</i>	-0.774	<i>Average</i>	-0.577	<i>Average</i>	-1.095
T. Murry	-0.698	A. Miller	-0.490	T. Harris	-1.023
K. Irving	-0.689	C. Miles	-0.486	M. Beasley	-1.022
S. Livingston	-0.679	H. Thompson	-0.483	M. Williams	-1.002
J. Jack	-0.665	D. Waiters	-0.481	M. Teletovic	-0.998
J. Holiday	-0.656	D. Wade	-0.480	Z. Randolph	-0.977

TABLE 5

Basis 5. Shot efficiency (top table) and frequency (bottom table). We list the top and bottom five defenders in terms of the effect on the log-odds on a shooters' shot efficiency from center three (basis 5). Negative effects imply that the defender decreases the log-odds of an outcome, relative to the global average player (zero effect). The three columns consist of defenders in the three groups listed in Figure 6 and the respective group means. Kawhi Leonard, who is a highly regarded perimeter defender, ranks top five in defensive impact on both shot frequency and efficiency in this basis.

in median distance (relative to the average defender) to the offender in region b . A defender's overall effect on the outcome of a shot depends on how close he tends to be to the shooter at the moment the shot is taken, as well as the players' specific defensive skill parameter ϕ_j . Again, smaller values correspond to a reduction in the shooter's shot efficiency, with negative values implying a defender that is better than the global average.

First, as a key point, we illustrate that defenders can affect shot frequency (where an offender shoots) and shot efficiency (whether the basket is made) and that, crucially, these represent distinct characteristics of a defender. This is best illustrated via two well regarded defensive centers, Dwight Howard and Roy Hibbert. Table 4 includes effects for defenders in the restricted area (basis 1). Roy Hibbert ranks first in his effect on shot efficiency in this region. Dwight Howard, however, ranks only 85 out of 138 (amongst similar defenders). In

shot selection, however, Dwight Howard ranks fourth in his suppression of shot attempts in the restricted area whereas Roy Hibbert ranks 121 out of 138. In the deep paint (basis 2) the dichotomy is even more striking: Hibbert ranks fourth in reducing efficiency, whereas Howard ranks 126th. In frequency, Howard ranks first, whereas Hibbert is 122nd. This demonstrates that skilled defenders may impact the game in different ways, as a result of team defensive strategy and individual skill. Figure 9 clearly depicts the contrasting styles of these players.

The defender effects do not always diverge so drastically between shot efficiency and frequency, however. Some defenders, are effective at reducing both shot frequency and efficiency. For instance, Kawhi Leonard, a well regarded perimeter defender, ranks in the top five in reducing both shot frequency and shot efficiency for center threes (basis 5) (Table 5).

Importantly, our model is informative about how opposing shooters perform against any defender in any region of the court. Even if a defender rarely defends shots in a particular region, they may still be partly responsible for giving up the shot in that region. For example, as a point guard, Chris Paul defends relatively few shots in basis 1, yet he is the best at reducing shot attempts in this area compared to other point guards (Table 4), likely in large part because he gets so many steals. As a defender he spends very little time in this court space, but we are still able to estimate how often his man beats him to the basket for a shot attempt.

Finally, it is possible to use this model to infer the best defensive matchups. Specifically, we can infer the expected points per possession a player should score if he were defended by a particular defender. Fittingly, we found the best defender on LeBron James is Kawhi Leonard. Leonard received a significant attention for his tenacious defense on James in the 2013 NBA finals. Seemingly, when the Heat play the Spurs and when James faces Leonard, we expect James to score fewer points per possession than he would against any other player.

While our results yield a detailed picture of individual defensive characteristics, each defender’s effect should only be interpreted in the context of the team they play with. Certainly, Leonard would not come out so favorably if he didn’t play on one of the better defensive teams in the league. Moreover, how much a point guard reduces opposing shot attempts in the paint may depend largely on whether that defender plays with an imposing center. Since basketball defense is inherently a team sport, isolating marginal individual effects is likely not possible without a comprehensive understanding of both team defensive strategy and a model for the complex interactions between defenders. Nevertheless, our model provides detailed summaries of individual player effects in the context of their current team— a useful measure in its own right.

6. Discussion

In this paper, we have shown that by carefully constructing features from optical player-tracking data, one is able to fill a current gap in basketball analytics – defensive metrics. Specifically, our approach allows us to characterize how players

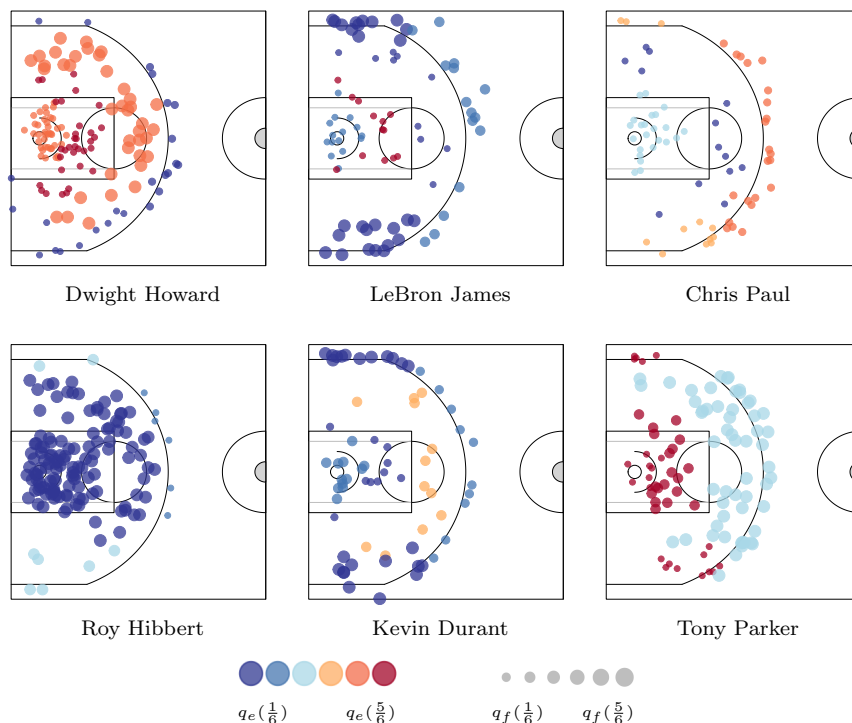


FIG 9. *Defensive shot charts.* The dots represent the locations of the shots faced by the defender, the color represents how the defender changes the expected shot efficiency of shots, and the size of the dot represents how the defender affects shot frequency, in terms of the efficiency quantiles q_e and frequency quantiles q_f . Hibbert and Howard’s contrasting defensive characteristics are immediately evident. Not surprisingly, Chris Paul, the league leader in steals, reduces opponents’ shot frequency everywhere on the court.

affect both shooting *frequency* and *efficiency* of the player they are guarding. By using an NMF-based decomposition of the court, we find an efficient and data-driven characterization of common shot regions which naturally corresponds to common basketball intuition. Additionally, we are able to use this spatial decomposition to simply characterize the spatial shot and shot-guarding tendencies of players, giving a natural low-dimensional representation of a player’s shot chart. Further, to learn who is guarding whom we build a spatio-temporal model which is fit with a combination of the EM-algorithm and generalized least squares, giving simple closed-form updates for inference. Knowing who is guarding whom allows for understanding of which players draw significant attention, opening the court up for their teammates. Further, we can see which teams induce a significant amount of defensive switching, allowing us to characterize the chaos induced by teams both offensively and defensively.

Combining this court representation and the mapping from offensive to defensive players, we are able to learn how players inhibit (or encourage) shot attempts in different regions of the court. Further, conditioned on a shot being

taken, we study how the defender changes the probability of the shot being made.

Moving forward, we plan to use our results to understand the effects of coaching by exploring the spatial characteristics and performance of players before and after trades or coaching changes. Similarly, we intend to look at the time-varying nature of defensive performance in an attempt to understand how players mature in their defensive ability.

References

- Dankmar Böhning. Multinomial logistic regression algorithm. *Annals of the Institute of Statistical Mathematics*, 44(1):197–200, 1992.
- Jean-Philippe Brunet, Pablo Tamayo, Todd R Golub, and Jill P Mesirov. Meta-genes and molecular pattern discovery using matrix factorization. *Proceedings of the National Academy of Sciences of the United States of America*, 101.12: 4164–9, 2004.
- Dan Cervone, Alexander D’Amour, Luke Bornn, and Kirk Goldsberry. Point-wise: Predicting points and valuing decisions in real time with NBA optical tracking data. 2014.
- Noel Cressie. *Statistics for spatial data*, volume 900. Wiley New York, 1993.
- Andrew Gelman and Donald B Rubin. Inference from iterative simulation using multiple sequences. *Statistical science*, pages 457–472, 1992.
- Kirk Goldsberry. Courtvision: New visual and spatial analytics for the NBA. MIT Sloan Sports Analytics Conference, 2012.
- Kirk Goldsberry. The Dwight effect: A new ensemble of interior defense analytics for the NBA. MIT Sloan Sports Analytics Conference, 2013.
- John Frank Charles Kingman. *Poisson Processes*. Oxford university press, 1992.
- Justin Kubatko, Dean Oliver, Kevin Pelton, and Dan T Rosenbaum. A starting point for analyzing basketball statistics. *Journal of Quantitative Analysis in Sports*, 3(3):1–22, 2007.
- Daniel D. Lee and H. Sebastian Seung. Learning the parts of objects by non-negative matrix factorization. *Nature*, 401(6755):788–791, 1999.
- Daniel D. Lee and H. Sebastian Seung. Algorithms for non-negative matrix factorization. *Advances in Neural Information Processing Systems (NIPS)*, 13:556–562, 2001.
- Brian Macdonald. A regression-based adjusted plus-minus statistic for NHL players. *Journal of Quantitative Analysis in Sports*, 7(3):4, 2011.
- Andrew C. Miller, Luke Bornn, Ryan Adams, and Kirk Goldsberry. Factorized point process intensities: A spatial analysis of professional basketball. In *Proceedings of the 31st International Conference on Machine Learning (ICML)*, 2014.
- Jesper Møller, Anne Randi Syversveen, and Rasmus Plenge Waagepetersen. Log Gaussian Cox processes. *Scandinavian Journal of Statistics*, 25(3):451–482, 1998.
- Kevin Murphy. *Machine Learning: A Probabilistic Perspective*. The MIT Press, 2012.

- Iain Murray and Ryan Prescott Adams. Slice sampling covariance hyperparameters of latent gaussian models. In *NIPS*, pages 1732–1740, 2010.
- Iain Murray, Ryan P. Adams, and David J.C. MacKay. Elliptical slice sampling. *Journal of Machine Learning Research: Workshop and Conference Proceedings (AISTATS)*, 9:541–548, 2010.
- Dan T Rosenbaum. Measuring how nba players help their teams win. *82Games.com* (<http://www.82games.com/comm30.htm>), pages 4–30, 2004.
- Yunus Saatchi. *Scalable Inference for Structured Gaussian Process Models*. PhD thesis, University of Cambridge, 2011.
- Joseph Sill. Improved NBA adjusted plus-minus using regularization and out-of-sample testing. In *Proceedings of the 2010 MIT Sloan Sports Analytics Conference*, 2010.
- Stan Development Team. Stan: A C++ library for probability and sampling, version 2.2, 2014. URL <http://mc-stan.org/>.
- AC Thomas, Samuel L Ventura, Shane T Jensen, Stephen Ma, et al. Competing process hazard function models for player ratings in ice hockey. *The Annals of Applied Statistics*, 7(3):1497–1524, 2013.